Computational Study on a HS- Sensing Reaction Utilizing a Pyrylium Derivative

ARTICLE *in* THE JOURNAL OF PHYSICAL CHEMISTRY A · MAY 2012

Impact Factor: 2.69 · DOI: 10.1021/jp300353y · Source: PubMed

2 AUTHORS:

Yinghong Sheng
Florida Gulf Coast University
35 PUBLICATIONS **414** CITATIONS
SEE PROFILE

Yi Ren
Sichuan University
67 PUBLICATIONS **768** CITATIONS
SEE PROFILE

THE JOURNAL OF PHYSICAL CHEMISTRY A

Article

pubs.acs.org/JPCA

Computational Study on a HS^- Sensing Reaction Utilizing a Pyrylium Derivative

Yinghong Sheng*,† and Yi Ren*,‡

†Department of Chemistry & Mathematics, College of Arts & Sciences, Florida Gulf Coast University, 10501 FGCU Boulevard, South, Fort Myers, Florida 33965, United States

‡College of Chemistry, and Key State Laboratory of Biotherapy, Sichuan University, Chengdu 610064, People's Republic of China

Supporting Information

ABSTRACT: In this paper, we present a comprehensive computational study on the hydrogen sulfide sensing mechanism in aqueous solution using a pyrylium derivative. The possible sensing mechanisms were investigated under the neutral condition and acidic condition in the gas phase and in aqueous solution. The pyrylium−thiopyrylium transformation under the neutral condition is thermodynamically unfavorable, while it is greatly facilitated in the acidic condition catalyzed by a hydronium cation. In addition, the UV−vis absorption maxima of pyryliums and thiopyryliums were investigated at the TDDFT/B3LYP/6-31G+(d,p) level. The red shift of absorption maximum from unsubstituted pyrylium and thiopyrylium to dimethylamino-subisituted pyrylium and thiopyrylium as well as the red shift seen in the pyrylium−thiopyrylium transformation is interpreted in terms of the molecular orbital theory.

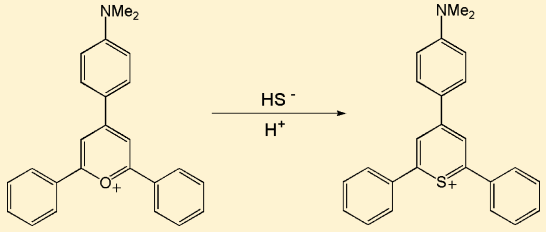

1. INTRODUCTION

Hydrogen sulfide is found naturally in coal pits, sulfur springs, oil, and gas wells. Hydrogen sulfide is released primarily as a gas and spreads in the air. However, in some instances, it may be released in the liquid waste in the form of hydrogen sulfide HS^-. Both hydrogen sulfide and sulfide anion present serious hazards to the health of living organisms when encountered in elevated concentrations. Therefore, the detection and sensing of hydrogen sulfide or sulfide anion is of great interest. Most of the determination procedures so far face problems related with the necessity of reaching a high sensitivity free of interferences, such as methylene blue method.[1] Ion chromatography using special separation resins and a suppressor column coupled to a number of detection systems, such as conductometric,[2] electrochemical,[3] ion-selective electrode,[4] photometric,[5] and ICP-MS,[6] has been a commonly used tool for separation and detection of sulfide ions from complex matrixes. However, most of these procedures are expensive and not suitable for in situ or at site determinations. There has been emerging interest in using chromogenic-sensing molecules for the colorimetric and selective detection of anions.[7] However, most chromogenic reagents for anion detection only work in organic solvents.[8] Jimenez et al.[9] reported a new chromogenic-sensing pyrylium salt (*para*-dimethylamino-2,4,6-triphenylpyrylium) for the colorimetric and selective detection of the hydrogen sulfide anion in aqueous solution.

Pyrylium salts belong to a very important class of cationic organic molecules. Pyrylium cations are related to benzene by replacement of a CH by an O^+ ion, and they are more reactive than benzene but stable; therefore, these molecules are of considerable practical interest and are very useful in chemical synthesis.[10] Pyrylium salts have been widely used as sensitizers for photoinduced electron-transfer (PET) reactions[11] and photocatalysts.[12] A number of works have focused on the development of sensors for anions,[13] amines,[14] amino acids,[15] peptoids,[16] ATP,[17] proteins,[18] as well as mercury(II) ion.[19] Pyrylium salts have also been implemented in applications in nonlinear optical (NLO) materials and power-limiting optical data storage.[20] The compounds synthesized from reactions involving 2,4,6-trimethylpyrylium have been used as therapeutic[21] and anticancer agents.[22]

In the presence of a hydrogen sulfide anion, *para*-dimethylamino-2,4,6-triphenylpyrylium is transformed into thiopyrylium (see Scheme 1), with the maximal absorption red-shifting from 540 nm for *para*-dimethylamino-2,4,6-triphenylpyrylium to 580 nm for the *para*-dimethylamino-2,4,6-triphenylthiopyrylium derivative. Only the hydrogen

Scheme 1. Pyrylium to Thiopyrylium Transformation

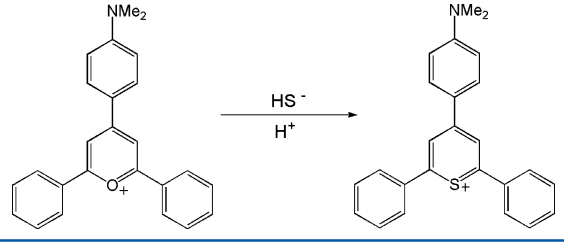

Received: January 11, 2012
Revised: May 12, 2012
Published: May 14, 2012

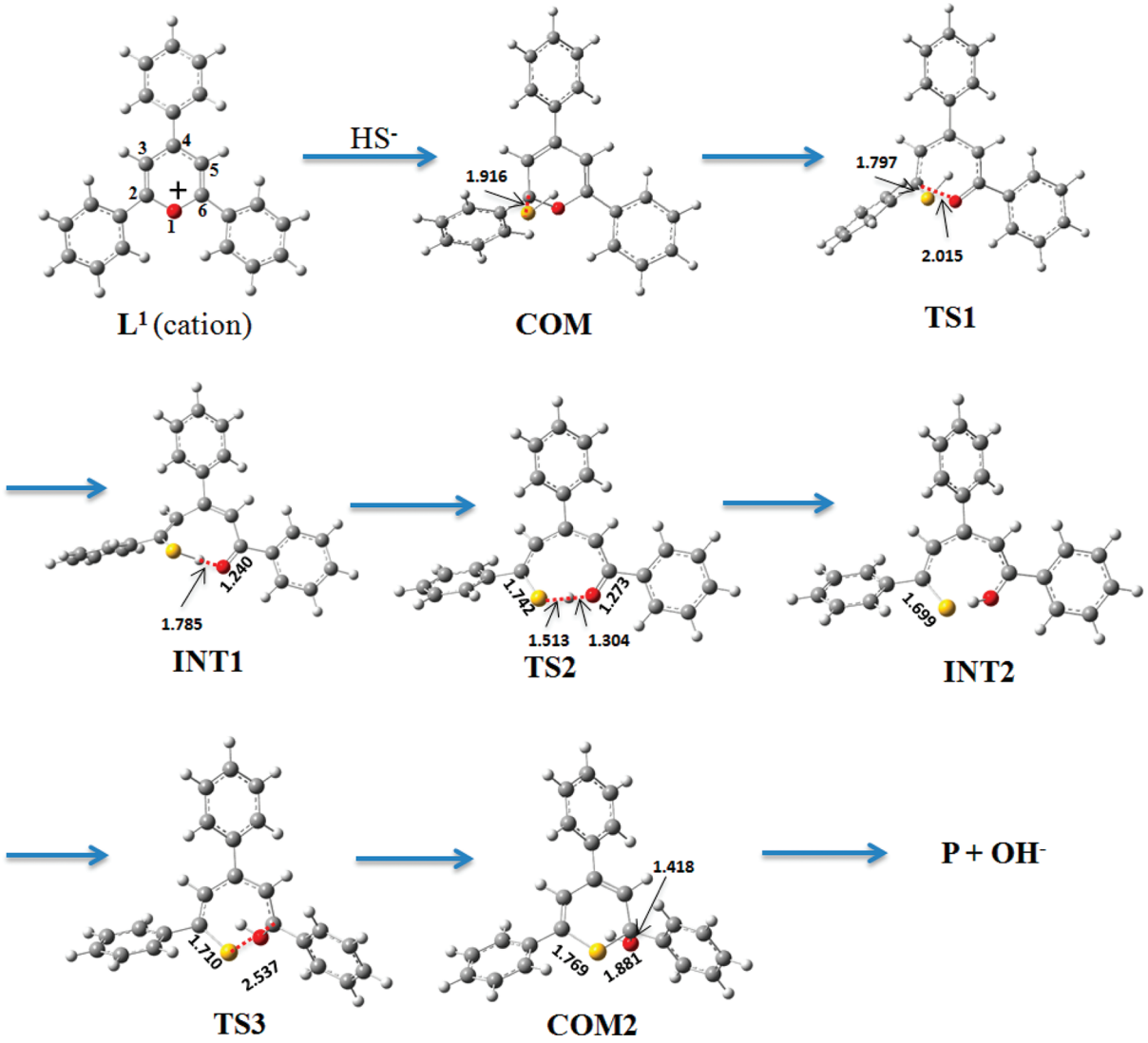

Figure 1. The B3LYP/6-31G(d) optimized complexes, intermediates, transition structures, and product for reaction between 2,4,6-triphenylpyrylium and hydrogen sulfide anion.

sulfide anion gives a color change from magenta to blue; this makes this pyrylium−thiopyrylium transformation highly specific in responding to the hydrogen sulfide anion and could be used for the qualitative determination of the sulfide anion in water. Therefore, in this work, we reported a comprehensive computational study on the hydrogen sulfide sensing mechanism using the pyrylium derivative. The possible reaction mechanism in the neutral condition was investigated. For comparison, the reaction mechanism in the acidic condition was also studied, providing the insight on how hydronium affects the reaction mechanism and catalyzes the pyrylium−thiopyrylium transformation. In addition, the substituent and solvent effects on the UV−vis spectral maximal absorption shifting during the reaction were also investigated.

2. CALCULATION METHODS AND THE MODEL COMPOUNDS

The choice of theoretical level depends on the accuracy requested and the size of a molecule. Density functional theory has been demonstrated to predict excellent molecular geometries.[23] Therefore, the possible reaction mechanisms were studied using the B3LYP nonlocal density functional approximation.[24] The geometries of reactants, products, transition states, and intermediates were optimized by means of the Berny approach, a modified Schlegel method.[25] Vibrational frequency calculations were performed to confirm whether the obtained geometry represents a transition or minimum-energy structure.

The 6-31G(d) basis set is a good compromise between efficiency and accuracy[26] and has been proven to reproduce well the molecular parameters. The further expansion of the basis set has less impact on the accuracy of the molecular geometries.[27] Therefore, we will report the results obtained from the 6-31G(d) basis set unless otherwise mentioned.

The reactions to which the theoretical models are compared were conducted in aqueous solutions. The solvent effect on the reaction mechanism was taken into account by single-point energy calculations using the CPCM polarizable conductor solvation model.[28] In order to mimic the experimental conditions, the dielectric constant of $\varepsilon = 78.36$ (corresponding to water) was used.

The UV−vis absorption was computed at the time-dependent density functional theory (TDDFT/B3LYP) level employing the 6-31G+(d,p) basis set using the B3LYP/6-31G(d) optimized geometries.[29] The solvent effect on UV−vis spectra was

dx.doi.org/10.1021/jp300353y | J. Phys. Chem. A 2012, 116, 5420−5427

investigated using the CPCM polarizable conductor calculation model.

The TDDFT calculations were performed on both 2,4,6-triphenylpyrylium and amino-substituted 2,4,6-triphenylpyrylium and their analogs. In order to save computer time, 2,4,6-triphenylpyrylium was used as the model compound to study the reaction mechanisms. All of the calculations were carried out using the Gaussian 03 program.[30]

3. RESULTS AND DISCUSSION

A. Pyrylium−Thiopyrylium Transformation in Neutral Conditions. The B3LYP/6-31G(d) optimized complexes, intermediates, transition structures, and product for reaction between 2,4,6-triphenylpyrylium and hydrogen sulfide anion are shown in Figure 1. The calculated relative energies of the species involved in the pyrylium−thiopyrylium transformation in the gas phase and in aqueous solution can be found in Table 1.

Table 1. B3LYP/6-31G(d) Calculated Relative Energies (kcal/mol) of the Species Involved in the Pyrylium−Thiopyrylium Transformations in the Gas Phase and in Aqueous Solution

species	gas phase	aqueous solution
	Under Neutral Condition	
$\mathbf{L^1 + SH^-}$	0.00	0.0
COM	−105.3	−26.3
TS1	−83.9	−6.7
INT1	−99.9	−24.3
TS2	−98.1	−21.9
INT2	−101.7	−25.3
TS3	−90.3	−15.0
COM2	−103.9	−26.7
P + OH^-	77.6	45.3
	Under Acidic Condition	
$\mathbf{L^1 + SH^- + H_3O^+}$	0.00	0.0
COM−H_3O^+	−157.4	−99.2
TS1−H_3O^+	−157.3	−98.0
INT1−H_3O^+	−182.4	−121.7
TS2−H_3O^+	−142.2	−88.0
P−2H_2O	−195.9	−139.5

Compound 2,4,6-triphenylpyrylium ($\mathbf{L^1}$) is a cation; the two C−O bond lengths in $\mathbf{L^1}$ are both 1.354 Å. Anionic HS^- attacks the C2 atom of the pyrylium ring, instead of the O1 atom, and forms a complex (**COM**). This is consistent with the Mulliken charge distribution calculation in which the charges on O1, C2, C3, C4, C5, and C6 are −0.477e, +0.340e, −0.222e, +0.139e, −0.222e, and +0.340e, respectively. In **COM**, the distance between S and C2 is 1.916 Å, and the O1−C2 and O1−C6 distances elongate to 1.428 and 1.368 Å, respectively; also, the C2−C3 bond length increases to 1.496 Å in **COM** from 1.379 Å in $\mathbf{L^1}$. This indicates that the S···C2 bond is partially formed in **COM**. The strong attraction between the pyrylium cation and hydrogen sulfide anion greatly stabilizes the formed complex (**COM**), and the energy stabilization amounts to −105.3 kcal/mol in the gas phase. When the solvent effect is considered, the energy stabilization decreases to −26.3 kcal/mol; this is due to that the solvent stabilization from a polar solvent on the charged $\mathbf{L^1}$ cation, and the HS^- anion is greater than on the neutral complex (**COM**).

The pyrylium ring-opening takes place on the O1−C2 bond. The corresponding transition structure (**TS1**) is shown in Figure 1. In **TS1**, the SH group forms a bond with the C2 atom; it breaks the O1−C2 bond. The S−C2 and O1···C2 distances amount to 1.797 and 2.015 Å, respectively. The O1−C6 becomes a double bond. The vibrational analysis confirms that **TS1** is the pyrylium ring-opening transition structure, with an imaginary frequency of −412.8 cm^{-1}. The activation energy is calculated to be 21.4 kcal/mol in the gas phase.

Following the pyrylium ring-opening, an intermediate (**INT1**) is formed. The phenyl ring on C2 rotates and becomes almost perpendicular to the opened pyrylium frame, and the C2−O1 distance further elongates to 3.205 Å. The Mulliken charge distribution shows that the hydrogen atoms of the newly attached SH and carbonyl oxygen atom carry +0.15e and −0.51e. This charge interaction leads to a shorter H···O distance (1.785 Å), stabilizing the intermediate as well as preparing the hydrogen atom to be transferred to the carbonyl group.

The hydrogen migration transition structure (**TS2**) is located and can be found in Figure 1. The migrating hydrogen atom lies in between the sulfur and oxygen atoms. The distances between the hydrogen atom and the sulfur and oxygen atoms amount to 1.513 and 1.304 Å, respectively. The S−C2 is shortened to 1.742 Å in **TS2**, while the C6═O1 bond is slightly elongated to 1.273 Å. The hydrogen migration only needs to overcome a 1.8 kcal/mol activation energy in the gas phase and leads to the second intermediate (**INT2**), where the carbonyl becomes the hydroxyl group.

The last step of pyrylium−thiopyrylium transformation is formation of the S−C6 bond, which leads to a thiopyrylium−OH complex (**COM2**), namely, **TS3**. In the transition structure, **TS3**, the S···C6 distance is shortened to 2.537 Å from 3.486 Å in **INT2**. The approaching of a sulfur atom toward C6 pushes the OH to the other side of the opened pyrylium ring. The activation energy for ring-closure is predicted to be around 11.3 kcal/mol in the gas phase.

After ring-closure, the S−C6 bond length becomes 1.881 Å because of the attached OH group, which is slightly longer than the regular S−C bond by about 0.1 Å. This attached OH group destroys the aromatic system of the four phenyl rings. In order for thiopyrylium to exhibit colorimetric change, the four rings must be conjugated; thus, the OH group must leave, in order for the C5−C6 to become a double bond. However, removing OH in the gas phase requires about 180.9 kcal/mol of energy; thus, the reaction would not likely take place. When the solvent effect was considered, the activation energies slightly changed, as shown in Figure 3 and Table 1. The energy changes of the reaction in both gas-phase calculations and solvent effect calculations imply that the pyrylium−thiopyrylium transformation would not happen due to the extremely high endothermic last step. Therefore, in the following section, the reaction mechanism in acidic conditions will be investigated.

B. Pyrylium−Thiopyrylium Transformation in Acidic Conditions. The reaction mechanism under acidic conditions is found to be totally different from that under neutral conditions. A hydronium ion is introduced to model the reaction under acidic conditions. The hydronium is found to form a strong hydrogen bond with the pyrylium oxygen atom, as shown in Figure 2. One proton departs from H_3O^+ and approaches the oxygen atom in the pyrylium ring. The distance between H and O1 amounts to 1.054 Å.

Similar to the reaction in neutral conditions, the HS^- attacks C2 and forms a complex, **COM−H_3O^+**. The H_3O^+ ion stabilizes the complex **COM−H_3O^+** by about 52 kcal/mol compared to the complex **COM** in the neutral conditions in the gas phase;

dx.doi.org/10.1021/jp300353y | J. Phys. Chem. A 2012, 116, 5420−5427

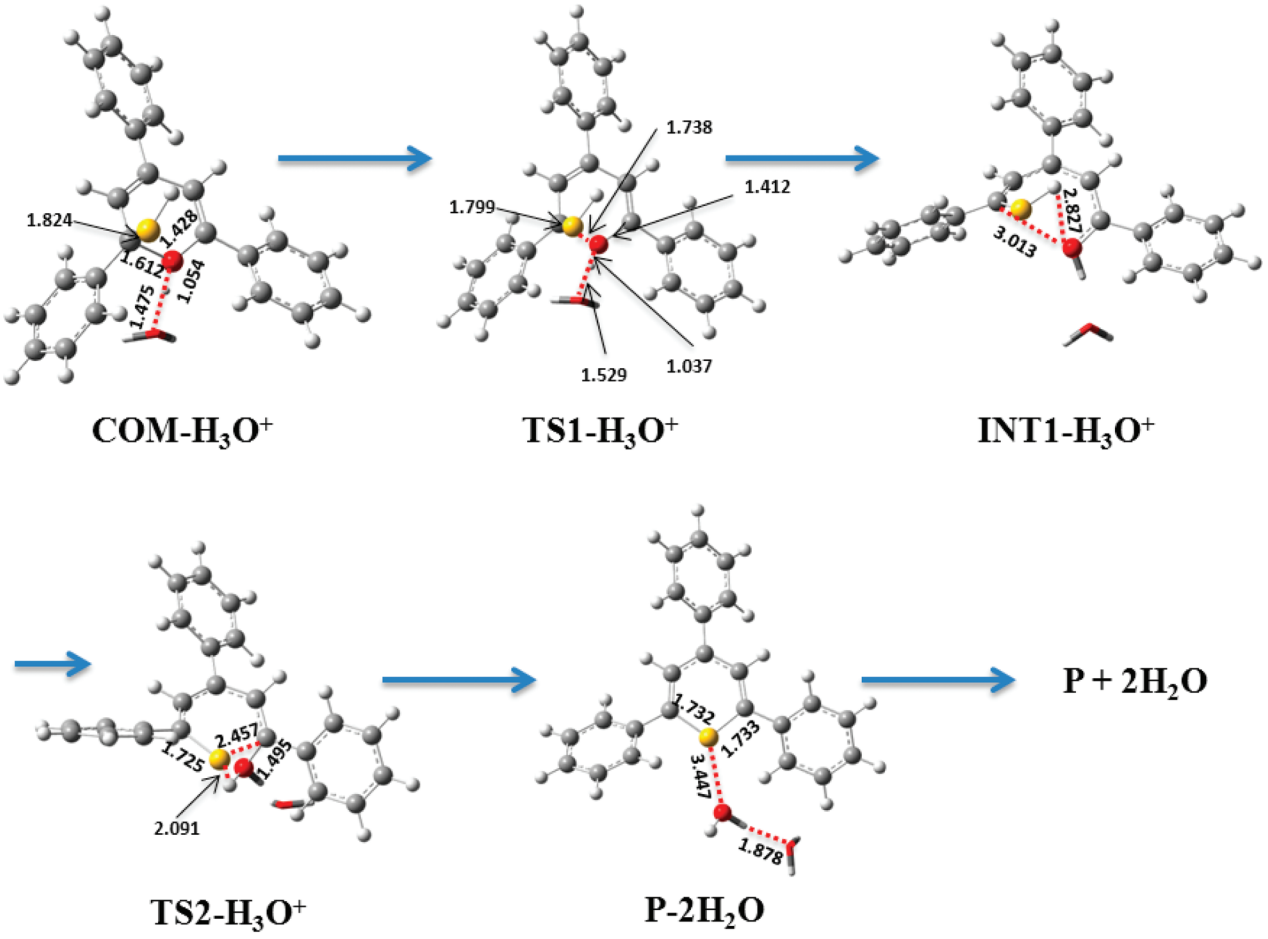

Figure 2. The B3LYP/6-31G(d) optimized complex, intermediate, transition structures, and product for the reaction between 2,4,6-triphenylpyrylium and hydrogen sulfide anion with the assistance of hydronium. The hydronium ion is shown in tube coloration; the other atoms follow standard CPK coloration.

when the solvent effect is considered, the energy stabilization amounts to 72.9 kcal/mol.

With the assistance of H_3O^+, the ring-opening is almost barrierless, and the activation energy amounts to only 0.17 kcal/mol in the gas phase. The solvent effect slightly increases the activation energy to 1.2 kcal/mol. The located ring-opening transition structure, **TS1−H_3O^+** is shown in Figure 2. As one can see that the ring-opening transition structure is a very early transition structure, the O1···C2 distance amounts to 1.738 Å, only 0.126 Å longer than that in the complex. The H_3O^+ in transition structure maintains a similar orientation with respect to the pyrylium ring seen in the complex, except that the hydronium proton moves slightly closer to the pyrylium oxygen, with the distance between H and O1 being 1.037 Å.

After the ring-opening, an intermediate **INT1−H_3O^+** results. The phenyl and SH groups on C2 rotate outward with respect to the newly formed OH group. In the meantime, the angles in the opened pyrylium frame increase. This leads to a longer distance, 3.502 Å, between C2 and C6. However, this step is necessary because it prepares the way for the hydrogen atom of SH to be transferred to the OH group, and then, sulfur can form a bond with C6 and finalize the ring-closure to thiopyrylium.

The H-migration from the sulfur atom to the oxygen atom and the S−C6 bond formation are found to take place simultaneously. The corresponding transition structure **TS2−H_3O^+** is shown in Figure 2. The vibrational frequency calculation indicates that the only one imaginary frequency, −339.6 cm^{-1}, corresponds to S···H−O1 and S···C6 stretching modes. The S···C6 distance amounts to 2.457 Å in **TS2−H_3O^+**. The O1−C6 bond length increases to 1.495 Å in **TS2−H_3O^+** from 1.318 Å in **INT1−H_3O^+**. The activation energy for the H-migration/ring-closure is predicted to be 40.2 kcal/mol in the gas phase. When the solvent effect is considered, the activation energy decreases to 33.7 kcal/mol (see Table 1). After the proton migrates to the hydroxyl group, a free water molecule is formed, and the pyrylium−thiopyrylium transformation is complete; product **P−2H_2O** results.

To compare two reaction mechanisms, the potential energy surfaces of the two reaction mechanisms in neutral and acidic conditions are charted together in Figure 3. From Figure 3, one can conclude that the reaction in the neutral conditions is a five-step reaction: (1) First, pyrylium forms a complex with HS^-; (2) then, the C2−O1 bond cleavage leads to the pyrylium ring-opening, followed by (3) H-migration from SH to carbonyl and (4) the formation of the S−C6 bond; last, (5) the leaving of the HO^- group leads to the thiopyrylium product. However, the reaction under the acidic conditions is a three-step reaction, including (1) forming a complex from pyrylium, the hydrogen sulfide anion, and the hydronium cation, (2) ring-opening, and (3) H-migration/ring-closure to the product.

The reaction under neutral conditions is highly endothermic and therefore thermodynamically unfavorable. The energy

dx.doi.org/10.1021/jp300353y | J. Phys. Chem. A 2012, 116, 5420−5427

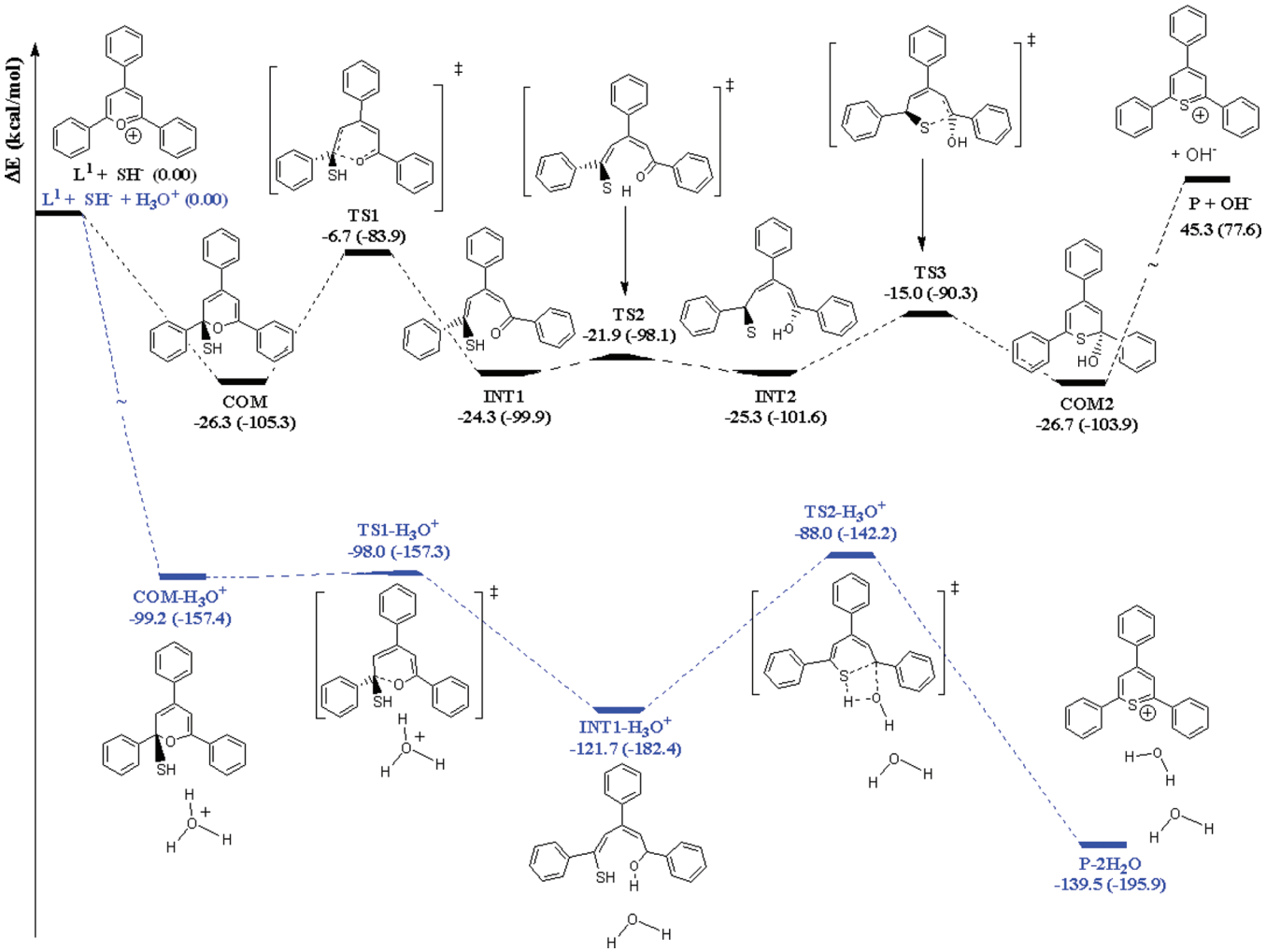

Figure 3. The potential energy surfaces for the pyrylium−thiopyrylium transformation of 2,4,6-triphenylpyrylium in the neutral and acidic solutions. The relative energies in aqueous solution and in the gas phase (in parentheses) are in kcal/mol.

change of the reaction under neutral conditions amounts to 45.3 kcal/mol in aqueous solution, while the energy change for the reaction in the acidic aqueous solution amounts to −139.5 kcal/mol; therefore, the pyrylium−thiopyrylium transformation is greatly thermodynamically favored in the acidic conditions. The hydronium effectively catalyzes the transformation by forming a free water molecule using the proton and hydroxyl group, making the reaction in the acidic conditions quite feasible.

c. UV−vis Spectra Maximal Absorption. The TDDFT calculation at the B3LYP/6-31+G(d,p) level has been prove to reproduce reasonable excitation energies,[31] therefore the UV−vis Spectra of pyryliums and thiopyryliums were studied at the TDDFT/B3LYP/6-31G+(d,p) level using the B3LYP/6-31G(d) optimized structures. The solvent effect on UV−vis spectra were investigated using the CPCM polarizable conductor calculation model.

In the literature, both experimental and theoretical studies have been performed on the absorption spectra of a series of 2,6-dimethyl-4-arylpyrylium salts, and the changes in absorption of these pyrylium salts[32] were explained using the *x,y*-band notation[33] developed by Balaban and co-workers. Another experimental and theoretical results shows that the counterion might affect the optical properties of pyryliums.[34] To clarify the effect of the counterion on the absorption maxima of the pyryliums under investigation in this work, we performed full geometry optimizations with the counterion included (BF_4^- used as the counterion). The distance between the pyrylium/thiopyrylium ring oxygen or sulfur atom and the negatively charged counterion amounts to 3.401 and 3.299 Å, respectively for *para*-dimethylamino-2,4,6-triphenylpyrylium tetrafluoroborate and *para*-dimethylamino-2,4,6-triphenylthiopyrulium tetrafluoroborate. The TDDFT/B3LYP/6-31+G(d,p) computed absorption maxima in aqueous solution amount to 493 and 530 nm for *para*-dimethylamino-2,4,6-triphenylpyrulium tetrafluoroborate and *para*-dimethylamino-2,4,6-triphenylthiopyrylium tetrafluoroborate, respectively. However, the absorption maxima without the counterion in aqueous solution amount to 488 and 526 nm, respectively. The inclusion of the counterion exhibits a similar red shift (37 nm) for pyrylium−thiopyrylium transformation as that in the absence of the counterion (38 nm). In both cases, the calculated red shifts are in excellent agreement with the experimental value (40 nm). Therefore, in this section, we only discuss the changes in the absorption maxima without the counterion.

Table 2 shows the TDDFT/B3LYP/6-31+G(d,p) computed HOMO, LUMO energy levels, band gaps, and absorption maxima (λ_{max}) of *para*-dimethylamino-2,4,6-triphenylpyrylium, *para*-dimethylamino-2,4,6-triphenylthiopyrulium, 2,4,6-triphenylpyrylium, and 2,4,6-triphenylthiopyrulium.

dx.doi.org/10.1021/jp300353y | J. Phys. Chem. A 2012, 116, 5420−5427

Table 2. Computed HOMO, LUMO Energies, Band Gaps, Dipole Moments, Maximal Absorption, Oscillator Strength, and Excitation Type of the Pyryliums and Thiopyryliums in the Aqueous State and in the Gas Phase (in Parentheses)

species	amino-pyrulium	amino-thiopyrylium	pyrulium	thiopyrylium
HOMO (au)	−0.2002 (−0.3149)	−0.1995 (−0.3127)	−0.3632	−0.3658
LUMO (au)	−0.0987 (−0.2159)	−0.1063 (−0.2212)	−0.2375	−0.2427
Band Gap (eV)	2.76 (2.69)	2.53 (2.49)	3.42	3.35
μ(Debye)	5.14 (4.15)	5.29 (4.27)	0.51	0.33
λ_{max} (nm)	488 (464)	526 (497)	413	431
f	1.067 (0.962)	0.984 (0.853)	0.373	0.337
excitation	$\pi-\pi^*$ ($\pi-\pi^*$)	$\pi-\pi^*$ ($\pi-\pi^*$)	$\pi-\pi^*$	$\pi-\pi^*$

For 2,4,6-triphenylpyrylium, the $S_0 \rightarrow S_1$ transition is primarily the HOMO−LUMO transition; this transition is much weaker than that of dimethylamino-substituted triphenylpyrylium. From Figure 4b, one can see that the HOMO orbital of 2,4,6-triphenylpyrylium is localized at the 2- and 6-phenyl rings; the LUMO has its electron density largely localized on the pyrylium rings. The HOMO orbital has nodal planes on the *y*-axis, while the LUMO orbital has nodal planes along the *x*-axis. This significantly weakens the HOMO−LUMO transitions; thus, the corresponding oscillator strength amounts to 0.373. The absorption maximum is calculated to be 413 nm. For 2,4,6-triphenylthiopyrulium, the shapes of the HOMO and LUMO orbitals (Figure 4d) are quite similar to those of 2,4,6-triphenylpyrulium, except that the LUMO orbital coefficients are slightly more localized at the thiopyrylium ring. This replacement of the O by S atom slightly lowers the HOMO−LUMO gap to 3.35 eV, and consequently, a longer absorption maximum of 431 nm results.

For *para*-dimethylamino-2,4,6-triphenylpyrulium, the shape of the LUMO orbital (Figure 4a) is similar to that of unsubstituted 2,4,6-triphenylpyrulium (Figure 4b). However, the HOMO orbital is quite different, with the major orbital coefficients localized at the amino group and the 4-phenyl group. Both HOMO and LUMO orbitals have nodal planes on the *x*-axis; therefore, the HOMO−LUMO transition is strongly allowed. Therefore, the TDDFT/B3LYP/6-31+G(d,p) computed UV−vis spectrum exhibits a very strong absorption at 488 nm. The corresponding oscillator strength amounts to 1.067. This transition is synonymous with Balaban's *y*-band notation. The dimethylamino group is an electron-donating group, which lowers the HOMO−LUMO gap. This rationalizes the longer absorption maximum for dimethylamino-substituted pyrylium than that for 2,4,6-triphenylpyrulium.

The HOMO and LUMO orbitals (Figure 4c) of *para*-dimethylamino-2,4,6-triphenylthiopyrylium in aqueous solution show similar features to Figure 4a; thus, the HOMO−LUMO transition is also strongly allowed, with an oscillator strength of 0.984. Comparing the molecular orbital energy levels between *para*-dimethylamino-2,4,6-triphenylpyrulium and thiopyrylium, the difference in HOMO energy levels amounts to 0.02 eV, while the difference in LUMO energy levels amounts to 0.21 eV. The replacement of the sulfur atom in the pyrylium ring lowers the LUMO level more in thiopyrylium than that in pyrylium; this results in a lower band gap (2.53 eV) for *para*-dimethylamino-2,4,6-triphenylthiopyrylium than that of *para*-dimethylamino-2,4,6-triphenylpyrylium (2.75 eV). Because the transition in thiopyrylium requires less energy, the absorption maximum in aqueous solution red shifts from 488 nm for *para*-dimethylamino-2,4,6-triphenylpyrulium to 526 nm for *para*-dimethylamino-2,4,6-triphenylthiopyrylium.

4. CONCLUSION

In this paper, we presented a comprehensive computational study on the sulfide sensing mechanism using a pyrylium derivative, that is, the pyrylium−thiopyrylium transformation. The possible sensing mechanisms were investigated. Under the

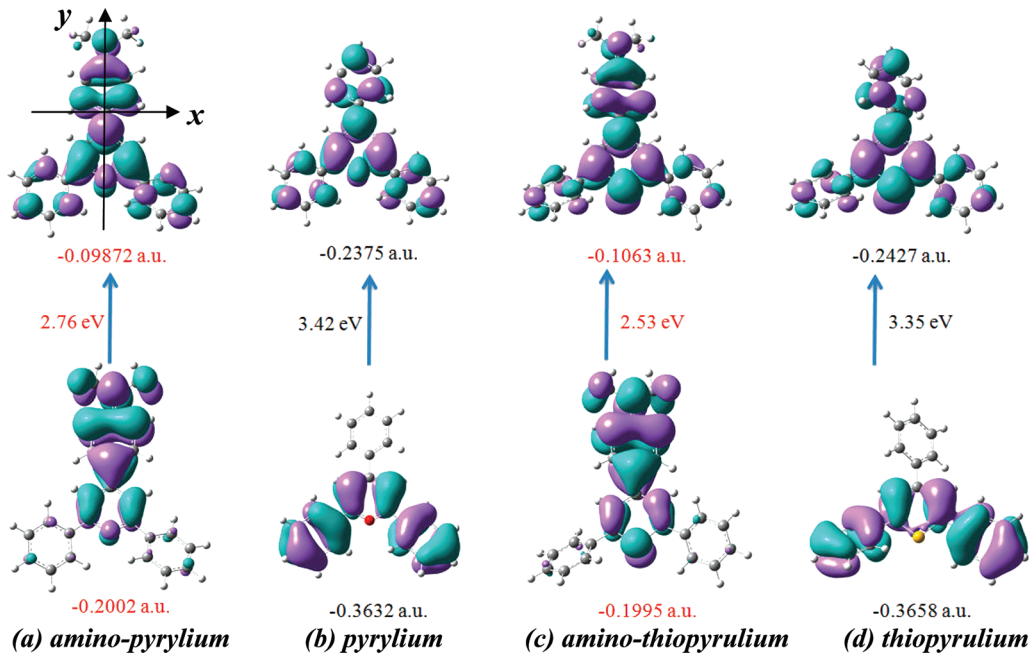

Figure 4. The HOMO, LUMO molecular orbitals for (a) *para*-dimethylamino-2,4,6-triphenylpyrylium, (b) 2,4,6-triphenylpyrylium, (c) *para*-dimethylamino-2,4,6-triphenylthiopyrulium, and (d) 2,4,6-triphenylthiopyrulium at the B3LYP/6-31+G(d,p) level.

dx.doi.org/10.1021/jp300353y | J. Phys. Chem. A 2012, 116, 5420−5427

neutral condition, the reaction is a five-step reaction: (1) First, pyrylium forms a complex with HS^-; (2) C−O bond cleavage occurs, leading to ring-opening; (3) H-migration occurs from SH to carbonyl followed by (4) formation of a S−O bond to ring-closure and (5) leaving of the HO^- group. The reaction under the acidic condition is a three-step reaction: (1) forming of a complex from pyrylium, the hydrogen sulfide anion, and the hydronium cation, (2) pyrylium ring-opening, and (3) H-migration/ring-closure to the product. Under neutral conditions, the pyrylium−thiopyrylium transformation is thermodynamically unfavorable, while it is greatly facilitated in the acidic conditions catalyzed by the hydronium cation.

The UV−vis absorption maxima of pyryliums and thiopyryliums were investigated at the TDDFT/B3LYP/6-31G+(d,p) level. The red shift of the absorption maximum from unsubstituted pyrylium and thiopyrylium to amino-subisituted pyrylium and thiopyrylium, as well as the red shift seen in the pyrylium−thiopyrylium transformation, is interpreted in terms of the molecular orbital theory. The TDDFT calculation indicated that the replacement of the sulfur group in the pyrylium ring lowers the LUMO level more in thiopyrylium than that in pyrylium and results in a lower band gap (2.53 eV) for *para*-dimethylamino-2,4,6-triphenylthiopyrylium than that for *para*-dimethylamino-2,4,6-triphenylpyrylium (2.75 eV), corresponding to a red shift of 37 nm in aqueous solution. This is in excellent agreement with the experimental value of 40 nm.

■ ASSOCIATED CONTENT

Ⓢ Supporting Information

Table 1S lists the B3LYP/6-31G(d) calculated total energies (au) of the spieces involved in the pyrylium−thiopyrylium transformation in the gas phase and in the aqueous solution. The full list of authors for ref 30 is also listed. This material is available free of charge via the Internet at http://pubs.acs.org.

■ AUTHOR INFORMATION

Corresponding Author

*E-mail: ysheng@fgcu.edu (Y.S.); yiren57@hotmail.com (Y.R.).

Notes

The authors declare no competing financial interest.

The authors declare no competing financial interest.

■ ACKNOWLEDGMENTS

This research was supported by the College of Arts & Sciences, Florida Gulf Coast University.

■ REFERENCES

(1) (a) Silva, M. P. S. P.; da Silva, I. S.; Abate, G.; Masini, J. C. *Talanta* **2001**, *53*, 843−850. (b) Tang, D.; Santshi, P. H. *J. Chromatogr., A* **2000**, *883*, 305−309. (c) Spazoani, M. A.; Davis, J. L.; Tinani, M.; Carroll, M. K. *Analyst* **1997**, *122*, 1555−1557.

(2) Weiss, J.; Gobl, M. *Fresenius' Z. Anal. Chem.* **1985**, *320*, 439−444.

(3) (a) Giuriati, C.; Cavalli, S.; Gorno, A.; Badacco, D.; Pastore, P. *J. Chromatogr., A* **2004**, *1023*, 105−112. (b) Han, K.; Koch, W. F. *Anal. Chim.* **1987**, *59*, 1016.

(4) Wang, W.; Chen, Y.; Wu, M. *Analyst* **1984**, *109*, 281−286.

(5) Miura, Y.; Matsushita, Y.; Haddad, P. R. *J. Chromatogr., A.* **2005**, *1085*, 47−53.

(6) Divjak, B.; Goessler, W. *J. Chromatogr., A* **1999**, *844*, 161−169.

(7) (a) Beer, P. D.; Gale, P. A. *Angew. Chem., Int. Ed.* **2001**, *40*, 486−516. (b) Gale, P. A. *Coord. Chem. Rev.* **2001**, *213*, 79−128. (c) Amendola, V.; Fabbrizzi, L.; Mangano, C.; Pallavicini, P.; Poggi, A.; Taglietti, A. *Coord. Chem. Rev.* **2001**, *219*−*221*, 821−837. (d) Wiskur, S. L.; Ait-Haddou, H.; Lavigne, J. J.; Anslyn, E. V. *Acc. Chem. Res.* **2001**, *34*, 963−972.

(8) (a) Amendola, V.; Bastianello, E.; Fabbrizzi, L.; Mangano, C.; Pallavicini, P.; Perotti, A.; Manotti-Lanfredi, A.; Ugozzoli, F. *Angew. Chem., Int. Ed.* **2000**, *39*, 2917−2920. (b) Hayashita, T.; Honodera, T.; Kato, R.; Nishizawa, S.; Teramae, N. *Chem. Commun.* **2000**, 755−756. (c) Han, M. S.; Kim, D. H. *Angew. Chem., Int. Ed.* **2002**, *41*, 3809−3811.

(9) (a) Jimenez, D.; Martinez-Mañez, R.; Sancenon, F.; Ros-Lis, J. V.; Benito, A.; Soto, J. *J. Am. Chem. Soc.* **2003**, *125*, 9000−9001. (b) Zakrzewski, R.; Ciesielski, W.; Ulanowska, A.; Martinez-Mañez, R. *Phosphorus, Sulfur Silicon Relat. Elem.* **2009**, *184*, 1139−1148.

(10) (a) Balaban, A. T.; Fischer, G. W.; Dinculescu, A.; Koblik, A. V.;Dorofeenko, G. N.; Mezheritskii, V. V.; Schroth, W. In *Pyrylium Salts: Synthesis, Reactions and Physical Properties*; Advances in Heterocyclic Chemistry, Supplement 2; Katrisky, A. R., Ed.; Academic Press: New York, 1982. (b) Balaban, T. S.; Balaban, A. T. In *Science of Synthesis; Houben−Weyl Methods of Molecular Transformations*; Thomas, D. E., Ed.; Georg Thieme Verlag: Stuttgart, Germany, Vol. *14*, 2003; pp 11−200. (c) Bell, J. R.; Franken, A.; Garner, C. M. *Tetrahedron* **2009**, *65*, 9368−9372. (d) Müller, C.; Vogt, D. *C. R. Chimie* **2010**, *13*, 1127−1143. (e) Ba, F.; Poul, P. L.; Guen, R. L.; Cabon, N.; Caro, B. *Tetrahedron Let.* **2010**, *51*, 605−608.

(11) (a) Sadhiya Banu, I.; Ramamurthy, P. *J. Photochem. Photobiol., A* **2009**, *201*, 175−182. (b) Che, Y.; Ma, W.; Ji, H.; Zhao, J.; Ling, Z. *J. Phys. Chem. B* **2006**, *110*, 2942−2948. (c) Latour, V.; Pigot, T.; Simon, M.; Cardy, H.; Lacombe, S. *Photochem. Photobiol. Sci.* **2005**, *4*, 221−229. (d) Halder, M. *Chem. Phys.* **2004**, *303*, 243−253. (e) Sanjuan, A.; Pillai, M. N.; Alvaro, M.; Garcia, H. *Chem. Phys. Lett.* **2001**, *341*, 153−160. (f) Khairutdinov, R. F.; Hurst, J. K. *J. Am. Chem. Soc.* **2001**, *123*, 7352−7359. (g) Miranda, M. A.; Garcia, H. *Chem. Rev.* **1994**, *94*, 1063−1089. (h) Aprile, C.; Martin, R.; Alvaro, M.; Garcia, H.; Scaiano, J. C. *Chem. Mater.* **2009**, *21*, 884−890.

(12) (a) Arques, A.; Amat, A. M.; Santos-Juanes, L.; Vercher, R. F.; Marín, M. L.; Miranda, M. A. *Catal. Today* **2009**, *144*, 106−111. (b) Bayarri, B.; Carbonell, E.; Gimenez, J.; Esplugas, S.; Garcia, H. *Chemosphere* **2008**, *72*, 67−74. (c) Bonesi, S. M.; Carbonell, E.; Garcia, H.; Fagnoni, M.; Albini, A. *Appl. Catal., B* **2008**, *79*, 368−375. (d) Miranda, M. A.; Izquierdo, M. A.; Perez-Ruiz, R. *J. Phys. Chem. A* **2003**, *107*, 2478−2482. (e) Haberl, U.; Steckhan, E.; Blechert, S.; Wiest, O. *Chem.—Eur. J.* **1999**, *5*, 2859−2865. (f) Amat, A. M.; Arques, A.; Bossmann, S. H.; Braun, A. M.; Miranda, M. A.; Vercher, R. F. *Catal. Today* **2005**, *101*, 383−388. (g) Amat, A. M.; Arques, A.; Bossmann, S. H.; Braun, A. M.; Goeb, S.; Miranda, M. A.; Oliveros, E. *Chemosphere* **2004**, *57*, 1123−1130. (h) Alvaro, M.; Carbonell, E.; Fornes, V.; Garcia, H. *New J. Chem.* **2004**, *28*, 631−639.

(13) (a) Chernova, R. K.; Yastrebova, N. I.; Ivanova, M. A. *J. Anal. Chem.* **2006**, *61*, 230−235. (b) Martínez-Máñez, R.; Sancenón, F.; Soto, J. *Chem. Commun.* **2005**, 2790−2792.

(14) (a) Gómez-Valdemoro, A.; Martínez-Máñez, R.; Sancenón, F.; Garciá, F. C.; Garciá, J. M. *Macromolecules* **2010**, *43*, 7111−7121. (b) Garcia-Acosta, B.; Comes, M.; Bricks, J. L.; Kudinova, M. A.; Kurdyukov, V. V.; Tolmachev, A. I.; Descalzo, A. B.; Marcos, M. D.; Martínez-Máñez, R.; Moreno, A.; Sancenón, F.; Soto, J.; Villaescusa, L. A.; Rurack, K.; Barat, J. M.; Escriche, I.; Amorós, P. *Chem. Commun.* **2006**, 2239−2241. (c) Comes, M.; Marcos, M. D.; Martínez-Máñez, R.; Sancenón, F.; Soto, J.; Villaescusa, L. A.; Amorós, P.; Beltran, D. *Adv. Mater.* **2004**, *16*, 1783−1786.

(15) (a) Moghimi, A.; Maddah, B.; Yari, A.; Shamsipur, M.; Boostani, M.; Fall Rastegar, M.; Ghaderi, A. R. *J. Mol. Struct.* **2005**, *752*, 68−77. (b) Moghimi, A.; Rsstegar, M. F.; Ghandi, M.; Taghizadeh, M.; Yari, A.; Shamsipur, M.; Yap, G. P. A.; Rahbarnoohi, H. *J. Org. Chem.* **2002**, *67*, 2065−2074.

(16) Rudat, B.; Birtalan, E.; Thomé, I.; Kölmel, D. K.; Horhoiu, V. L.; Wissert, M. D.; Lemmer, U.; Eisler, H.-J.; Balaban, T. S.; Bräse, S. *J. Phys. Chem. B* **2010**, *114*, 13473−13480.

(17) Sancenón, F.; Descalzo, A. B.; Martínez-Máñez, R.; Miranda, M. A.; Soto, J. *Angew. Chem., Int. Ed.* **2001**, *40*, 2640−2643.

(18) Wetzl, B. K.; Yarmoluk, S. M.; Craig, D. B.; Wolfbeis, O. S. *Angew. Chem., Int. Ed.* **2004**, *43*, 5400−5402.

(19) Yari, A.; Abdoli, H. A. *J. Hazard. Mater.* **2010**, *178*, 713−717.

(20) (a) Polyzos, I.; Tsigaridas, G.; Fakis, M.; Giannetas, V.; Persephonis, P.; Mikroyannidis, J. *J. Phys. Chem. B* **2006**, *110*, 2593−2597. (b) Polyzos, I.; Tsigaridas, G.; Fakis, M.; Giannetas, V.; Persephonis, P. *Opt. Lett.* **2005**, *30*, 2654−2656. (c) Fakis, M.; Tsigaridas, G.; Polyzos, I.; Giannetas, V.; Persephonis, P.; Spiliopoulos, I.; Mikroyannidis, J. *Chem. Phys. Lett.* **2001**, *342*, 155−161. (d) Zhou, Y.-F.; Feng, S.-Y. *ChemPhysChem* **2002**, *3*, 969−972. (e) Alvaro, M.; Aprile, C.; Benitez, M.; Bourdelande, J. L.; Garcia, H.; Herance, J. R. *Chem. Phys. Lett.* **2005**, *414*, 66−70. (f) Purvinis, G.; Priambodo, P. S.; Pomerantz, M.; Zhou, M.; Maldonado, T. A.; Magnusson, R. *Opt. Lett.* **2004**, *29*, 1108−1110. (g) Nakayama, H.; Sugihara, O.; Okamoto, N.; Sate, H.; Mizuno, A.; Matsushima, R. *J. Opt. Soc. Am. B* **1998**, *15*, 477−483.

(21) (a) Dave, K.; Ilies, M. A.; Scozzafava, A.; Temperini, C.; Vullo, D.; Supuran, C. T. *Bioorg. Med. Chem. Lett.* **2011**, *21*, 2764−2768. (b) Güzel, Ö.; Maresca, A.; Scozzafava, A.; Salman, A.; Balaban, A. T.; Supuran, C. T. *Bioorg. Med. Chem. Lett.* **2009**, *19*, 2931−2934. (c) Gong, W.-T.; Li, X.-C.; Ning, G.-L.; Zhu, L.; Wang, L.; Lin, Y. *Spectrochim. Acta, Part A* **2005**, *62*, 835−839.

(22) Kovacic, P. *Curr. Med. Chem.: Anti-Cancer Agents* **2005**, *5*, 501−506.

(23) (a) Bauschlicher, C. W. *Chem. Phys. Lett.* **1995**, *246*, 40−44. (b) El-Azhary, A. A.; Suter, H. U. *J. Phys. Chem.* **1996**, *100*, 15056−15063.

(24) (a) Lee, C.; Yang, W.; Parr, R. *Phys. Rev. B* **1988**, *37*, 785−789. (b) Becke, A. D. *J. Chem. Phys.* **1993**, *98*, 5648−5652. (c) Miehlich, B.; Savin, A.; Stoll, H.; Preuss, H. *J. Chem. Phys.* **1989**, *90*, 5622−5629. (d) Stephens, P. J.; Devlin, F. J.; Chabalowski, C. F.; Frisch, M. J. *J. Phys. Chem.* **1994**, *98*, 11623−11627.

(25) Schlegel, H. B. *J. Comput. Chem.* **1982**, *3*, 214−218.

(26) (a) Sheng, Y.; Leszczynski, J.; Garcia, A.; Rosario, R.; Gust, D.; Springer, J. *J. Phys. Chem. B* **2004**, *108*, 16233−16243. (b) Holmén, A.; Broo, A. *Int. J. Quantum Chem.* **1995**, *22*, 113−122.

(27) (a) Hariharan, P. C.; Pople, J. A. *Chem. Phys. Lett.* **1972**, *16*, 217−219. (b) Hehre, W. J.; Radom, L.; Schleyer, P. v. R.; Pople, J. A. *Ab Initio Molecular Orbital Theory*; Wiley: New York, 1986.

(28) (a) Barone, V.; Cossi, M. *J. Phys. Chem. A* **1998**, *102*, 1995−2001. (b) Cossi, M.; Rega, N.; Scalmani, G.; Barone, V. *J. Comput. Chem.* **2003**, *24*, 669−681.

(29) (a) Bauernschmitt, R.; Ahlrichs, R. *Chem. Phys. Lett.* **1996**, *256*, 454−464. (b) Straman, R. E.; Scuseria, G. E.; Frisch, M. J. *J. Chem. Phys.* **1998**, *109*, 8218−8224.

(30) Frisch, M. J.; Trucks, G. W.; Schlegel, H. B.; Scuseria, G. E.; Robb, M. A.; Cheeseman, J. R.; Montgomery, Jr., J. A.; Vreven, T.; Kudin, K. N.; Burant, J. C.; et al. *Gaussian 03*, revision C.02; Gaussian, Inc.: Wallingford, CT, 2004.

(31) Sheng, Y.; Leszczynski, J.; Nguyen, T.-Q.; Bamgbelu, A. *Struct. Chem.* **2007**, *18*, 827−832.

(32) (a) Manoj, N.; Ajayakumar, G.; Gopidas, K. R.; Suresh, C. H. *J. Phys. Chem. A* **2006**, *110*, 11338−11345. (b) Manoj, N.; Gopidas, K. R. *J. Photochem. Photobiol., A* **1999**, *127*, 31−37. (c) Manoj, N.; Ajit Kumar, R.; Gopidas, K. R. *J. Photochem. Photobiol., A* **1997**, *109*, 109−118.

(33) Rulliére, C.; Declemy, A.; Balaban, A. T. *Can J. Phys.* **1985**, *63*, 191.

(34) (a) Jha, P. C.; Luo, Y.; Polyzos, I.; Persephonis, P.; Ågren, H. *J. Chem. Phys.* **2009**, *130*, 174312/1−174312/7. (b) Polyzos, I.; Tsigaridas, G.; Fakis, M.; Giannetas, V.; Persephonis, P.; Mikroyannidis, J. *Chem. Phys. Lett.* **2003**, *369*, 264−268.